

Supporting Information

**Revealing the Full Potential of CsPbIBr₂ Perovskite Solar Cells:
Advancements Towards Enhanced Performance**

Mohammad Ismail Hossain^{1,8,†,*}, Md. Shahiduzzaman^{2,3,†,*}, Junayed Hossain Rafij⁴,
Asman Tamang⁸, Md. Akhtaruzzaman^{5,6}, Almohamadi Hamad^{5,6}, Jamal Uddin⁷,
Nowshad Amin⁴, Jean-Michel Nunzi^{2,9}, and Tetsuya Taima^{2,3}

¹Department of Electrical and Computer Engineering, University of California, Davis,
Davis, CA 95616, USA

²Nanomaterials Research Institute, Kanazawa University, Kakuma, Kanazawa 920-
1192, Japan

³Graduate School of Natural Science and Technology, Kanazawa University,
Kakuma, Kanazawa 920-1192, Japan

⁴Department of Electrical and Electronics Engineering, Universiti Tenaga
Nasional(@The Energy University), Kajang, Selangor 43000, Malaysia

⁵Department of Chemistry, Faculty of Science, The Islamic University of Madinah,
Madinah, Saudi Arabia

⁶Sustainability Research Center, Islamic University of Madinah,
Madinah, Saudi Arabia

⁷Center for Nanotechnology, Department of Natural Sciences, Coppin State
University, Baltimore, MD 21216, USA

⁸Research and Development, Meta Materials Inc. (META), Pleasanton, CA 94588,
USA

⁹Department of Physics, Engineering Physics and Astronomy, Queens University,
Kingston, ON K7L 3N6, Canada

* Corresponding authors

†: Authors equally contributed to the work

S1. Optical Modeling: Power Density, Quantum Efficiency, and Short-circuit Current Density Calculations

The FDTD optical simulation allows for determining electric field distribution within the perovskite solar cell (PSC) structure. Hence, the total electron-hole generation rate and power density profiles in the device can be calculated. The total generation rate (GR_{Total}) using electric field, $E(x,y,z)$ is calculated by

$$GR_{Total}(\lambda) = \varepsilon'' \int \frac{|E(x,y,z)|}{2 \times h} d\lambda$$

1

where, ε'' is the imaginary part of the relative permittivity, $\varepsilon_r = (n-ik)^2$, where n is the refractive index, and k is the extinction coefficient of the perovskite absorber. And h is the Planck's constant.

The time-averaged power density absorbed within the PSC structure can be computed by

$$Q(x,y,z) = \frac{1}{2} c \varepsilon_0 n \alpha |E(x,y,z)|^2$$

2

where, c is the speed of light in free space, ε_0 is the permittivity of free space, n is the refractive index of the material and E is the electric field distribution. α is the absorption coefficient which is related to extinction coefficient of the material as given by $\alpha = 4\pi k/\lambda$, where λ is the wavelength. Based on the power density, the quantum efficiency (QE) of the PSC is calculated by

$$QE(\lambda) = \frac{1}{P_{Opt}} \int Q(x,y,z) dx dy dz$$

3

where, P_{Opt} is the optical input power of the sun. The QE is defined as the ratio of photons absorbed by the perovskite layer divided by the total number of photons incident to the solar cell. Furthermore, photon absorption in the perovskite absorber only contributes to the QE, and photons absorbed by other layers are considered to be parasitic absorption. The short-circuit current density (J_{SC}) can be calculated by

$$J_{SC} = \frac{q}{hc} \int \lambda \times QE(\lambda) \times S(\lambda) d\lambda$$

4

where, q is the electron charge and $S(\lambda)$ is the solar spectral irradiance (AM1.5G). Photons absorbed by the perovskite layer contribute to the J_{SC} , and photons absorbed by all other layers do not.

S2. Electrical Modelling: Current-Voltage Relationship

In the FEM approach, non-linear Poisson's, continuity, and drift-diffusion equations are engaged for the calculations. The charge density (ρ) and the electron and hole current densities (J_n , and J_p , respectively) can be expressed by

$$\rho = q(n - p + N_D + N_A)$$

5

$$J_n = -q\mu_n nE + qD_n \frac{\partial n}{\partial x}$$

6

$$J_p = -q\mu_p pE - qD_p \frac{\partial p}{\partial x}$$

7

$$J = J_n + J_p$$

where, n and p are electron concentration and hole concentration, respectively. N_D and N_A are donor density and acceptor density, respectively. μ_n and μ_p are electron and hole mobilities, respectively. \mathbf{E} is the electric field. $D_{n,p} = \mu_{n,p}(kT/q)$ are electron and hole diffusion constants. The electron-hole pair generation rate was used as an optical input for the FEM simulation, which was realized from the FDTD optical simulation. The generation rate for electrons and holes was kept constant with the total generation rate ($G_{Total} = G_n = G_p$). Furthermore, both radiative recombination (R_{rad}) and non-radiative recombination, which are auger recombination (R_{auger}), Shockley-Read-Hall recombination (R_{SRH}), and surface recombination ($R_{surface}$) rates, were considered for the investigation. The close boundary conditions were applied to the simulation environment, where ITO or doped ZnO and Ag metal contacts were designated as anode and cathode, respectively. To attain the J–V curve, the voltage swipe ranged from 0 to 1.6 V with a step size of 0.02 V.

Next, the photovoltaic performance parameter values from the J-V characteristic curve can be determined. Afterward, the power conversion efficiency (PCE) and fill factor (FF) of the solar cell can be calculated by

$$PCE = \frac{P_{MPP}}{P_{incident}} = \frac{J_{SC} \times V_{OC} \times FF}{P_{incident}} \quad 8$$

$$FF = \frac{P_{MPP}}{P_{incident}} = \frac{J_{MPP} \times V_{MPP}}{J_{SC} \times V_{OC}} \quad 9$$

where, P_{MPP} is the power at the maximum power point (MPP) of the solar cells. J_{MPP} and V_{MPP} are short-circuit current density and open-circuit voltage at the maximum power point. V_{OC} is open-circuit voltage and J_{SC} is short-circuit current density.

Table S1. Electronic data of used materials in the perovskite solar cell.^{3, 4, 10-12}

Parameters	Materials				
	<i>ETM</i>		<i>Perovskite</i>	<i>HTM</i>	
	<i>SnO₂</i>	<i>Doped ZnO</i>	<i>CsPbIBr₂</i>	<i>Spiro-OMeTAD</i>	<i>NiO</i>
Bandgap, E_g (eV)	3.72	3.27	1.95	3	3.6
Electron affinity, χ (eV)	4.13	4.29	3.59	2.6	1.6
Dielectric Permittivity, ϵ_r	9	10	6.5	3	11.7
Conduction band effective density of states, N_C (cm ⁻³)	1×10^{19}	2.2×10^{18}	1.66×10^{19}	5×10^{19}	2.5×10^{20}
Valence band effective density of states, N_V (cm ⁻³)	1.8×10^{16}	1.8×10^{19}	5.41×10^{19}	1×10^{19}	2.5×10^{20}
Electron mobility, μ_n (cm ² /Vs)	20	100	50	2	1×10^{-3}
Hole mobility, μ_p (cm ² /Vs)	10	25	50	5	1×10^{-3}
Donor density, N_D (cm ⁻³)	1×10^{16}	1×10^{17}	0	0	0
Acceptor density, N_A (cm ⁻³)	0	0	5×10^{16}	1×10^{18}	5×10^{17}
Lifetime of electron, τ_n (s)	1×10^{-9}	1×10^{-9}	1×10^{-5}	1×10^{-9}	1×10^{-9}
Lifetime of hole, τ_p (s)	1×10^{-10}	1×10^{-10}	5×10^{-6}	1×10^{-10}	1×10^{-10}
Surface recombination velocity of	1×10^7	1×10^7	1×10^7	1×10^7	1×10^7

electrons, S_n (cm/s)					
Surface recombination velocity of holes, S_p (cm/s)	1×10^7	1×10^7	1×10^7	1×10^7	1×10^7

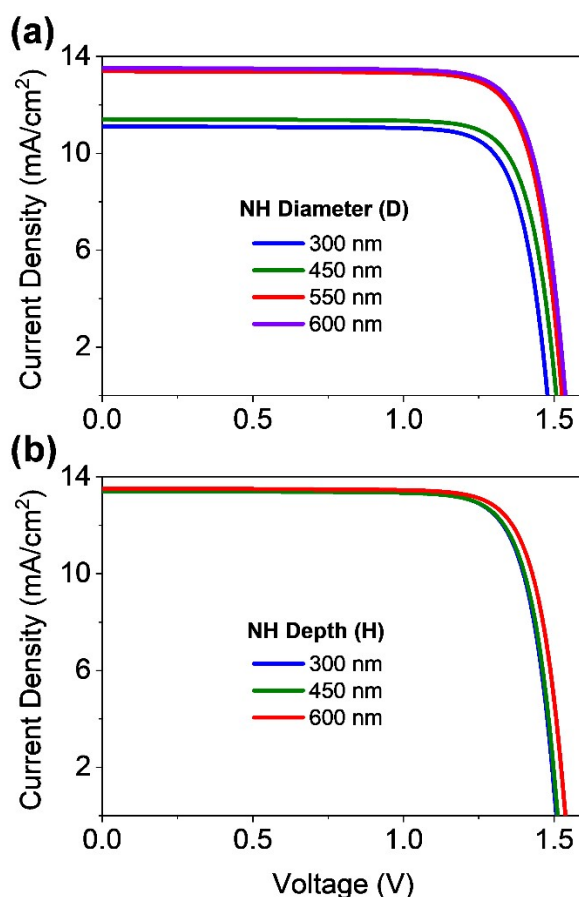


Figure S1. (a) Simulated J-V characteristic curves of the proposed PSCs for different nanohole (NH) diameters. The NH has a period of 600 nm and a depth of 600 nm. (b) Simulated J-V characteristic curves of the proposed PSCs for different nanohole (NH) depths. The NH has a period of 600 nm and a diameter of 550 nm.

Table S2. Effect of Nanohole diameter on the photovoltaic performance parameters of studied PSCs.

Nanohole Diameter	Photovoltaic Performance Parameters			
	J_{sc} (mA/cm ²)	V_{oc} (V)	FF (%)	PCE (%)
300 nm	11.10	1.45	80.5	12.95
450 nm	11.40	1.48	80.4	13.55

550 nm	13.40	1.53	80.6	16.44
600 nm	13.51	1.53	80.6	16.62

Table S3. Effect of Nanohole depth on the photovoltaic performance parameters of studied PSCs.

Nanohole Depth	Photovoltaic Performance Parameters			
	J_{sc} (mA/cm²)	V_{oc} (V)	FF (%)	PCE (%)
300 nm	13.37	1.52	80.6	16.37
450 nm	13.35	1.51	80.6	16.24
600 nm	13.4	1.53	80.6	16.50

References

1. M. I. Hossain, A. K. M. Hasan, W. Qarony, M. Shahiduzzaman, M. A. Islam, Y. Ishikawa, Y. Uraoka, N. Amin, D. Knipp, M. Akhtaruzzaman and Y. H. Tsang, *Small Methods*, 2020, **4**, 2000454.
2. M. I. Hossain, A. M. Saleque, S. Ahmed, I. Saidjafarzoda, M. Shahiduzzaman, W. Qarony, D. Knipp, N. Biyikli and Y. H. Tsang, *Nano Energy*, 2021, **79**, 105400.
3. Y. Da, Y. Xuan and Q. Li, *Sol. Energy Mater. Sol. Cells*, 2018, **174**, 206-213.
4. S. Sajid, A. M. Elseman, J. Ji, S. Dou, D. Wei, H. Huang, P. Cui, W. Xi, L. Chu, Y. Li, B. Jiang and M. Li, *Nanomicro Lett.*, 2018, **10**, 51.
5. S. Zandi and M. Razaghi, *Solar Energy*, 2019, **179**, 298-306.
6. P. Zhao, Z. Lin, J. Wang, M. Yue, J. Su, J. Zhang, J. Chang and Y. Hao, *ACS Appl. Energy Mater.*, 2019, **2**, 4504-4512.
7. L. M. Herz, *ACS Energy Lett.*, 2017, **2**, 1539-1548.
8. Q. Deng, Y. Li, L. Chen, S. Wang, G. Wang, Y. Sheng and G. Shao, *Mod. Phys. Lett. B*, 2016, **30**, 1650341.
9. T. Minemoto and M. Murata, *J. Appl. Phys.*, 2014, **116**, 054505.
10. M. Shahiduzzaman, M. I. Hossain, S. Visal, T. Kaneko, W. Qarony, S. Umezu, K. Tomita, S. Iwamori, D. Knipp, Y. H. Tsang, M. Akhtaruzzaman, J.-M. Nunzi, T. Taima and M. Isomura, *Nanomicro Lett.*, 2021, **13**, 36.
11. M. I. Hossain, M. Shahiduzzaman, S. Ahmed, M. R. Huqe, W. Qarony, A. M. Saleque, M. Akhtaruzzaman, D. Knipp, Y. H. Tsang, T. Taima and J. A. Zapien, *Nano Energy*, 2021, **89**, 106388.
12. M. I. Hossain, M. Shahiduzzaman, A. M. Saleque, M. R. Huqe, W. Qarony, S. Ahmed, M. Akhtaruzzaman, D. Knipp, Y. H. Tsang, T. Taima and J. A. Zapien, *Sol. RRL*. 2021, **5**, 2100509.